



# LUND UNIVERSITY

## Comparison of the chemical properties of iron and cobalt porphyrins and corrins.

Jensen, Kasper; Ryde, Ulf

*Published in:*  
ChemBioChem

*DOI:*  
[10.1002/cbic.200200449](https://doi.org/10.1002/cbic.200200449)

2003

*Document Version:*  
Peer reviewed version (aka post-print)

[Link to publication](#)

*Citation for published version (APA):*  
Jensen, K., & Ryde, U. (2003). Comparison of the chemical properties of iron and cobalt porphyrins and corrins. *ChemBioChem*, 4(5), 413-424. <https://doi.org/10.1002/cbic.200200449>

*Total number of authors:*  
2

*Creative Commons License:*  
Unspecified

### General rights

Unless other specific re-use rights are stated the following general rights apply:  
Copyright and moral rights for the publications made accessible in the public portal are retained by the authors and/or other copyright owners and it is a condition of accessing publications that users recognise and abide by the legal requirements associated with these rights.

- Users may download and print one copy of any publication from the public portal for the purpose of private study or research.
- You may not further distribute the material or use it for any profit-making activity or commercial gain
- You may freely distribute the URL identifying the publication in the public portal

Read more about Creative commons licenses: <https://creativecommons.org/licenses/>

### Take down policy

If you believe that this document breaches copyright please contact us providing details, and we will remove access to the work immediately and investigate your claim.

LUND UNIVERSITY

PO Box 117  
221 00 Lund  
+46 46-222 00 00

**Comparison of the chemical properties of  
iron and cobalt porphyrins and corrins**

**M. Sc. K. P. Jensen and Dr. U. Ryde**

*Department of Theoretical Chemistry*

*Lund University*

*Chemical Centre*

*P. O. Box 124*

*S-221 00 Lund*

*Sweden*

Correspondence to U. Ryde

E-mail: [Ulf.Ryde@teokem.lu.se](mailto:Ulf.Ryde@teokem.lu.se).

*Tel: +46-46-2224502*

*Fax: +46-46-2224543*

Density functional calculations have been used to compare various geometric, electronic, and functional properties of iron and cobalt porphyrins (Por) and corrins (Cor). The investigation is focused on octahedral  $M^{II/III}$  complexes (where M is the metal) with two axial imidazole ligands (as a model of *b* and *c* type cytochromes) or with one imidazole and one methyl ligand (as a model of methylcobalamin). However, we have also studied some five-coordinate  $M^{II}$  imidazole complexes and four-coordinate  $M^{I/II}$  complexes without any axial ligands as models of other intermediates in the reaction cycle of coenzyme B<sub>12</sub>. The central cavity of the corrin ring is smaller than that of porphine. We show that the cavity of corrin is close-to-ideal for low-spin  $Co^{III}$ ,  $Co^{II}$ , and  $Co^I$  with the axial ligands encountered in biology, whereas the cavity in porphine is better suited for intermediate-spin states. Therefore, the low-spin state of Co is strongly favoured in corrins, whereas there is a small energy difference between the various spin states in iron porphyrins. There are no clear differences for the reduction potentials of the octahedral complexes, but  $Co^ICor$  is more easily formed (by at least 40 kJ/mole) than  $Fe^IPor$ . Cobalt and corrin form a stronger Co-C bond that is more stable against hydrolysis than iron and porphine. Finally,  $Fe^{II/III}$  gives a much lower reorganisation energy than  $Co^{II/III}$ , owing to the occupied  $d_{z^2}$  orbital in  $Co^{II}$ . Altogether these results give some clues how Nature have chosen the tetra-pyrrole

rings and their central metal ion.

**Keywords:** cobalamin, haem, density functional theory, iron, porphyrin, vitamin B<sub>12</sub>

## Introduction

Two of the most remarkable chemical entities of living matter are the porphine and corrin rings. These two systems are vital for a tremendous amount of biochemical reactions, ranging from oxygen transport, electron transfer, and oxidative metabolism in the case of porphyrin,<sup>[1]</sup> to alkyl migration and methylation reactions in the case of corrin.<sup>[2-4]</sup> In spite of their differing functions, the structures are quite similar. The porphine ring has  $D_{4h}$  symmetry, with four pyrrole rings connected by methine bridges. As can be seen in Figure 1, the only two things that distinguish the two ring systems are the absence of one of the four methine bridges in corrin, a feature that lowers symmetry to  $C_{2v}$ , and ten saturated carbon atoms at the periphery of the corrin ring, which destroys the conjugation of the outer part of the ring and lowers the symmetry to  $C_1$ .

Nature seems to have a clear preference for iron as the central metal ion in porphyrin cofactors, whereas cobalt is normally found only in corrins. Among the first-row transition metals, cobalt has the lowest abundance in sea water together with scandium,<sup>[5]</sup> but still it is present in the ubiquitous coenzyme  $B_{12}$ . Cobalt resides between iron and nickel in the first row of the  $d$  block. It has common oxidation states of +II and +III, as does iron, but cobalt may even be reduced to a formal oxidation number of +I in vivo, a property that iron does not possess.<sup>[6]</sup> On the other

hand, iron porphyrins are well-known for their accessible high-valent states (formally  $\text{Fe}^{\text{IV}}$  and  $\text{Fe}^{\text{V}}$ ), which play an important role in the function of haem oxidases.<sup>[7]</sup>

The corrins exist in nature in the form of cobalamins. The  $\text{B}_{12}$  coenzymes contain a corrin ring with a  $d^6$  low spin  $\text{Co}^{\text{III}}$  ion in their octahedral resting states. In most cobalamin-dependent enzymes, the imidazole side chain of a histidine residue coordinates to the cobalt ion. In another group of enzymes, cobalt binds to the pendant dimethylbenzimidazole group of the coenzyme, the properties of which is quite similar to those of imidazole.<sup>[8]</sup> The second axial site is occupied by a methyl or 5'-deoxyadenosyl group, forming an organometallic Co-C bond. This bond is broken during the catalytic cycle, forming either a five-coordinate  $\text{Co}^{\text{II}}$  intermediate and an adenosyl radical, or a four-coordinate  $\text{Co}^{\text{I}}$  ion, where the imidazole ligand has dissociated and the methyl group has been transferred to a nucleophilic substrate.<sup>[2,9]</sup>

Haem enzymes show a larger variation in the axial ligands (His, Cys, Met, Tyr, Glu, Asp, amino terminal, or exogenous ligands), depending on the function.<sup>[9]</sup> The haem group can either be five-coordinate with an open coordination site, where a substrate binds, or six-coordinate with one or two ligands from the protein. However, the most common ligand is a histidine imidazole group, present for example in myoglobin, haemoglobin, peroxidases, haem oxygenase, and most

types of cytochromes.<sup>[10]</sup>

The aim of this paper is to study how the chemical properties of cobalt and iron, as well as porphyrin and corrin, differ. In particular, we want to understand why cobalt is associated with corrins and iron with porphyrins in nature. We have concentrated our study on one typical reaction for each of the two coenzymes, viz. the breakage of the Co-C bond, as a typical example of coenzyme B<sub>12</sub> metabolism, and electron transfer, as a typical example of the haem-containing cytochromes.

Several authors have addressed similar questions.<sup>[11-19]</sup> It has been suggested that corrin was selected to fit the smaller Co<sup>III</sup> ion.<sup>[11,13,19]</sup> Williams has proposed that low-spin Co<sup>II</sup> is unique among the available first-row transition metal ions to provide a stable and directed one-electron radical<sup>[17]</sup>. On the other hand, Pratt has attributed the choice of cobalt to the low 3d to 4s/4p promotion energy of Co<sup>II</sup>, which gives strong Co-C bonds, because the 3d orbitals are too small to form strong covalent bonds with carbon.<sup>[11,19]</sup> Moreover, he argues that corrin was chosen because it forms dimers with an appropriate Co-Co distance. Others have emphasised the flexibility of the corrin ring as an important factor in the labilisation of the Co-C bond.<sup>[14,15]</sup> Specifically, the mechanochemical trigger mechanism has been a major argument in favour of a specialised function of corrin systems, based on release of strain energy during

catalysis. However, recent experimental<sup>[20-22]</sup> and theoretical<sup>[23,24]</sup> results have indicated that such a conformational change is unlikely to drive a catalytic reaction within corrins. Finally, Rovira et al. have compared the geometric and electronic structure of four-coordinate cobalt corrin and porphine using theoretical calculations.<sup>[16]</sup> They show that the excitation energy associated with  $d_{x^2-y^2}$  occupation is much higher in corrins than in porphyrins.

Our investigation is based on similar density functional calculations. During recent years, such methods have successfully been applied to the study of both iron porphyrins<sup>[25-37]</sup> and coenzyme B<sub>12</sub> models.<sup>[16,24,38-42]</sup> Theoretical methods have the advantage of being cheap, fast, and giving pure results (well-defined reactions in vacuum). On the other hand, solvation effects and free energies are hard to describe in a consistent way, and the accuracy is limited. In this paper, we study how the geometry, thermodynamic stability, spin energies, electronic structure, reduction potential, reorganisation energy, and Co-C bond dissociation energy differ for iron and cobalt porphyrins and corrins. The results are discussed in relation to the earlier suggestions.

## **Results and Discussion**

### *Spin-splitting energies*

Several authors have suggested that porphine and corrin ligands were selected to make low-spin (LS) states available



for iron and cobalt, because the natural amino-acid ligands provide too weak a ligand field to drive iron or cobalt into the LS state.<sup>[13,17,43]</sup> This is probably most important for Co(II), for which the vast majority of ligands give rise to a high-spin (HS) state<sup>[13]</sup>. Moreover, it has been suggested that porphyrin was selected to keep iron close to the crossover point between the LS, intermediate-spin (IS), and HS states.  
[17]

In order to check these suggestions and to compare the relative strength of the porphine and corrin ligand fields and the intrinsic preferences of iron and cobalt, we have studied the energy differences between the LS, IS, and HS states of the octahedral Im-Me complexes (both M<sup>II</sup> and M<sup>III</sup>) and the square-pyramidal Im complexes (only M<sup>II</sup>), with all four combinations of Fe/Co and Por/Cor. All structures were fully geometry optimised. It should be noted that the calculated spin-splitting energies are appreciably less accurate than other estimates in this paper, because they are calculated as differences between different spin states, meaning that errors in the correlation energy are less likely to cancel. Yet, *differences* in spin-splitting energies between Fe and Co or Por and Cor should be reliable.

Unfortunately, it turned out that only one octahedral Im-Me complex was stable in the HS state, Fe<sup>II</sup>PorImMe. All the other complexes lost the imidazole ligand during the optimisation. The same applies also to the IS Co<sup>II</sup>CorImMe

complex (note that  $\text{Co}^{\text{II}}$  has seven  $d$  electrons and therefore does not have a sextet state comparable to the HS quintet state of  $\text{Fe}^{\text{II}}$ ). Therefore, only the energy difference between the LS and IS states is presented in Table 1.

For these octahedral Im-Me complexes, all combinations of metals and ring systems give rise to a LS ground state, in accordance with experimental results for cobalt corrins.<sup>[44]</sup> The IS states are 46-139 kJ/mole higher in energy for the  $\text{M}^{\text{III}}$  complexes. The difference is ~40 kJ/mole larger for Co than for Fe and also ~50 kJ/mole larger for Cor than for Por. The difference is slightly smaller for the  $\text{M}^{\text{II}}$  complexes, with a similar difference between Co and Fe. Thus, our calculations confirm that both Cor and Por give rise to strong ligand fields and that iron and porphine give complexes quite close to the spin-crossover point.

The spin-splitting energies of the five-coordinate Im complexes are even more interesting, because for these, we expect to find a difference in the preferred ground state. Experimentally, cob(II)alamin is LS, whereas five-coordinate  $\text{Fe}^{\text{II}}$  haem is normally HS, e.g. in deoxymyoglobin<sup>[7]</sup>. The results in Table 2 partly confirm this observation: The two cobalt complexes have LS ground states, with an energy difference of 21 (porphine) and 58 kJ/mole (corrin) to the IS states. However, for  $\text{Fe}^{\text{II}}$ PorIm, the calculations indicate that IS is actually 4 kJ/mole more stable than the HS state. Yet, this energy is so small that it may be caused by

deficiencies in the method or by the neglect of environmental effects. Similar results have been obtained in earlier calculations<sup>[35]</sup>. Clearly, the results confirm the shift of the ground state from LS.

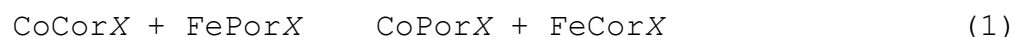
Similar results are also obtained for the four-coordinate  $M^I$  complexes. All these are most stable in the LS state. However, for the iron and porphine complexes, the IS and sometimes also the HS states are low-lying. Interestingly, the cobalt complexes are most stable in the open-shell singlet state, formed by antiferromagnetical coupling between  $Co^{II}$  and a ring radical. This has not been observed before<sup>[16]</sup>, but for  $Co^I Cor$ , the energy difference to the closed-shell LS state is only 4 kJ/mole, i.e. within the uncertainty of the method.

In conclusion, the spin-splitting energies indicate that cobalt and corrin favour the LS state, whereas Fe and Por give a small splitting between the various states. In the rest of this article we will study only model complexes in their electronic ground states.

#### *Thermodynamic stability*

Considering the *in vivo* abundance of iron porphyrins and cobalt corrins, it is natural to address the relative thermodynamic stability of these complexes. Stability considerations may explain why iron forms biological complexes with porphyrin rather than corrin, and that the

opposite is the case for cobalt. With theoretical means, we can calculate the reaction energy of the hypothetical isodesmic reaction:



where  $X$  represent various sets of axial ligands and all metals are in the same oxidation state,  $M^I$ ,  $M^{II}$ , or  $M^{III}$ . This reaction energy quantifies the change in energy obtained by replacing Co in the corrin ring with Fe from the porphine, and *vice versa*. The energy obtained for this reaction with various axial ligands and oxidation states of the metals are shown in Table 3. It can be seen that the reaction energies are quite small (8-22 kJ/mole) as are the solvation effects, 0-4 kJ/mole. In all except one case, the reaction energies are positive, indicating that the native combination of ions and ring systems is more stable than the alternative. However, for the Im-Me complexes with  $M^{II}$  ions, the reaction energy is negative, indicating that the non-native combination is more stable. This may be an effect of the differing electronic states for  $\text{Co}^{II}$  in these complexes (see below).

These energies include all chemical differences between the two ions and the two ring systems, e.g. ionic radii, chemical softness, and effective charge. However, they do not give any indication which of these properties may be important for the selection. Moreover, we expect that besides these thermodynamic preferences, there should also be some

*functional* reason for the selection of ions and ring systems. This will be investigated in the forthcoming sections.

#### *Geometries and the size of the ring cavities*

Next, we examine the geometries of the various complexes. In particular, we will discuss the size of the central cavity of the ring systems and compare it to the size of the ions, because it has been suggested that Cor was selected because its smaller cavity, which would fit  $\text{Co}^{\text{III}}$  properly.<sup>[11,13,19,45]</sup> The geometries of the optimised FePor and CoCor complexes are shown in Figure 2 (the corresponding CoPor and FeCor complexes are closely similar).

The metal-ligand distances of the optimised Im-Me and Im<sub>2</sub> models are collected in Tables 4 and 5, respectively. The M-C bond lengths are longer for iron (199-201 pm) than for the cobalt complexes (195-197 pm), but there is no significant difference between the Cor and Por rings.

The M-N<sub>Im</sub> distances vary more, which reflects that this bond is weaker and more flexible.<sup>[24]</sup> For the Im-Me complexes, the M-N<sub>Im</sub> bonds are rather long, 217-229 pm. They are longer for Fe than for Co and longer for Por than for Cor. For the Im<sub>2</sub> complexes, the two M-N<sub>Im</sub> distances are quite similar in length and shorter (198-209 pm) than in the Im-Me complexes. This is of course caused by the negative charge of the methyl ligand, which elongates the bonds of the other ligands, especially for the flexible Im ligand. However, in the  $\text{Co}^{\text{II}}$

complexes, the M-N<sub>Im</sub> bonds are very long (240–251 pm). The reason for this is that low-spin Co<sup>II</sup> is a d<sup>7</sup> ion, with an electron in the d<sub>z<sup>2</sup></sub> orbital, which is directed towards the axial ligands, thereby destabilising these interactions.

However, the most systematic differences are found for the equatorial M-N<sub>eq</sub> distances: Porphine has always ~9 pm longer M-N<sub>eq</sub> bonds (201–207 pm) than corrin (192–193 pm). On the other hand, these bonds show no clear trends with respect to the metal ion or oxidation states. This indicates that the M-N<sub>eq</sub> distances are mainly determined by the inherent size of the central cavity of the rings and can only barely be modified by the metal.

To test this, we calculated the trans N<sub>eq</sub>-N<sub>eq</sub> distance in free dianionic porphine. It is 417 pm after geometry optimisation. The corresponding distance in free anionic corrin is 395 pm (on average; the ring is distinctly non-planar with trans N<sub>eq</sub>-N<sub>eq</sub> distances of 377 pm and 413 pm). Thus, the cavity is 22 pm smaller in corrin than in porphyrin, owing to the missing methine bridge, in good accordance with the 9-pm difference found for the M-N<sub>eq</sub> bonds.

Thus, the differing cavity size can be an important factor in the selection of ions for the two ring systems. However, this cannot alone explain why cobalt is found in corrins and iron in porphyrins. On the contrary, the ionic radii for low-spin octahedral Fe<sup>III</sup> and Co<sup>III</sup> are equal (55

pm), whereas the ionic radius of  $\text{Co}^{\text{II}}$  (65 pm) is actually slightly larger for than that of  $\text{Fe}^{\text{II}}$  (61 pm).<sup>[44]</sup> Instead, it seems likely that the porphyrin ring was selected to allow other spin states than low spin; high-spin octahedral  $\text{Fe}^{\text{II}}$  and  $\text{Fe}^{\text{III}}$  have ionic radii of 78 and 65 pm, respectively.<sup>[44]</sup>

In order to test such a suggestion, we need to know the ideal bond length of iron and cobalt in porphyrin and corrin models with the particular ligands of interest. This can be studied by cutting the ring into two  $\text{NH}(\text{CH})_3\text{NH}^-$  moieties, as has been done before.<sup>[36]</sup> From Figure 3, it can be seen that such a model retains the number of carbon atoms in the chelate ring and the hybridisation of the ring systems, but it removes any restraints imposed by the ring system. Moreover, the same model is appropriate for both porphyrin and corrin, except for the additional charge, compared to corrin. Therefore, the optimum  $\text{M}-\text{N}_{\text{Im}}$  distances in models with this ligand can be expected to reflect the ideal bond length of that metal with the same axial ligands in a tetrapyrrole ring system.

We have optimised the structure of  $\text{M}(\text{NH}(\text{CH})_3\text{NH})_2\text{Im}_2$  with Co and Fe in both oxidation states. The results in Table 6 clearly illustrate the rigidity of the porphyrin and corrin rings. When the rings are broken, the  $\text{M}-\text{N}_{\text{eq}}$  distances change significantly. The  $\text{Fe}^{\text{II}}-\text{N}_{\text{eq}}$  distance is 199 pm, which is 4 pm longer than in corrin and 6 pm shorter than in porphyrin. The  $\text{Fe}^{\text{III}}-\text{N}_{\text{eq}}$  bonds are 194 pm, which is close to the bond

lengths found in corrin, but 9 pm shorter than in porphyrin. The difference between  $\text{Fe}^{\text{II}}$  and  $\text{Fe}^{\text{III}}$ , 5 pm, is close to the difference in ionic radii of the two ions, 6 pm, which shows that the calculations are reliable.

The  $\text{Co}^{\text{III}}\text{-N}_{\text{eq}}$  distance is the same as for  $\text{Fe}^{\text{III}}$ , 194 pm, in excellent agreement with their identical ionic radii. However, in porphyrin and corrin,  $\text{Co}^{\text{III}}$  gives 1-2 pm shorter bonds than does  $\text{Fe}^{\text{III}}$ , which indicates that  $\text{Co}^{\text{III}}$  forms stronger (more covalent) bonds than  $\text{Fe}^{\text{III}}$ . The  $\text{Co}^{\text{II}}\text{-N}_{\text{eq}}$  bonds in  $\text{Co}(\text{NH}(\text{CH})_3\text{NH})_2\text{Im}_2$  are 7 pm shorter than in porphyrin and 2 pm longer than in corrin.

Altogether, these results show that porphyrin and corrin form rather rigid ring systems, allowing for only small variations in the  $\text{M-N}_{\text{eq}}$  bond lengths. Interestingly, porphyrin with its double charge seems to be more flexible (201-207 pm) than the monanionic corrin ring (192-194 pm). The central cavity of porphyrin is appreciably larger (6-9 pm) than the ideal bond length of all ions considered in this investigation. This indicates that it would be ideal for ions with a radius of 62-67 pm (similar results have been obtained with other methods).<sup>[45]</sup> Thus, it would be ideal to the HS (65 pm) and IS states of  $\text{Fe}^{\text{III}}$  and close to ideal for HS  $\text{Co}^{\text{III}}$  (61 pm)<sup>[44]</sup> On the other hand, it is still too small for the (octahedral) HS states of  $\text{Fe}^{\text{II}}$  (78 pm) and  $\text{Co}^{\text{II}}$  (75 pm). This lends support to the suggestion that porphyrin was selected to allow various spin states of iron.



The central cavity of corrin is appreciably smaller than that of porphyrin. It is close to the ideal bond length of the LS state of all ions in this investigation (within 2 pm), except  $\text{Fe}^{\text{II}}$ , for which it is 5 pm too small. Thus, it is proper for ions with a radius of 54-56 pm. This means that the HS states of all ions are too large to fit properly into the cavity. Hence, the corrin ring, in contrast to porphyrin, selectively stabilises the LS states of the ions. Moreover, it fits excellently both  $\text{Co}^{\text{II}}$  and  $\text{Co}^{\text{III}}$ , but not  $\text{Fe}^{\text{II}}$ . Thus, corrin seems to be an ideal ligand for LS cobalt chemistry. This is most likely a strong reason why corrin is selected for cobalt chemistry, whereas porphyrin is employed in iron chemistry.

To see if the cavity size of corrin is appropriate also for the actual intermediates in the reaction cycles of coenzyme  $\text{B}_{12}$ , we have compared the  $\text{Co-N}_{\text{eq}}$  bond lengths of  $\text{Co}^{\text{III}}\text{CorImMe}$ ,  $\text{Co}^{\text{II}}\text{CorIm}$ , and  $\text{Co}^{\text{I}}\text{Cor}$  (LS states) with the corresponding complexes with the broken-ring ligand  $\text{NH}(\text{CH})_3\text{NH}$ . The results are also included in Table 6 and they show that the  $\text{Co-N}_{\text{eq}}$  distance increases by 2-3 pm when the corrin ring is broken in all three complexes. Therefore, we can conclude that the corrin ligand is close to optimal (within 3 pm) for all relevant oxidation states and ligands of LS cobalt, especially as B3LYP normally overestimates metal-ligand bond lengths by a few pm.<sup>[38]</sup>

We have also tested an alternative ring-broken model,

applicable for the corrin ring (with the correct single negative charge),  $M(\text{NH}(\text{CH})_3\text{NH})(\text{CH}_2\text{NH}(\text{CH})_2\text{NHCH}_2)$ , c.f. Figure 3. However, it turned out that this ligand was too crowded so that the two ring fragments do not always stay in the same plane and that the individual  $M\text{-N}_{\text{ax}}$  bond lengths differ strongly, e.g. two bonds of 190 pm and two of 206-208 pm for the  $\text{Fe}^{\text{III}}\text{Im}_2$  complex (for the  $\text{NH}(\text{CH})_3\text{NH}$  ligand, the individual bond lengths vary by less than 0.4 pm). Therefore, these results were judged to be less reliable, although they give a similar average  $M\text{-N}_{\text{ax}}$  bond length to  $\text{NH}(\text{CH})_3\text{NH}$  for most of the complexes.

Finally, we note that the present results also provide a qualitative explanation of the spin-splitting energies discussed above (c.f. Tables 1 and 2). Corrin is more rigid than porphyrin and has a cavity size close to that of low-spin states of all ions, except  $\text{Fe}^{\text{II}}$ . Therefore, the spin-splitting energies are appreciably larger for corrin than for porphyrin for all complexes, except  $\text{Fe}^{\text{II}}$ .

Interestingly, porphyrin ruffling has been invoked to explain how various metal ions may shorten the otherwise unfavourable, long Co-N bonds,<sup>[46]</sup> which result from the large cavity size of porphyrin.<sup>[47]</sup> However, as opposed to the ruffled ground state observed for sterically crowded Ni-porphyrins,<sup>[59]</sup> all porphyrin complexes investigated here are completely planar, regardless of spin state, as can be seen for the  $\text{FePor}$  complexes in Figure 2. Thus, the differing

cavity sizes of corrin and porphyrin are basic features of the planar systems.

Figure 2 also shows the structures of all the optimised CoCor complexes. These complexes are distinctly non-planar, as an effect of missing methine linkage and the saturated atoms in the ring system. The distortion of the corrin ring is normally measured as the fold angle, defined as the angle between the two average planes formed by the seven inner atoms in the corrin ring on both sides of a line from the missing methine link to the opposite methine atom.<sup>[2]</sup> It is 4-7° (lowest for the Im-Me complexes and largest for the Im-OH complexes) in the investigated complexes, without any systematic differences between iron and cobalt.

#### *Electronic structure*

In order to compare the electronic structures of the various complexes, we have calculated the Mulliken charges of various groups and atoms. These are collected in Tables 7 and 8 for the Im-Me and Im<sub>2</sub> complexes, respectively. They show that the charge on the metal ion (0.54-0.85 e) and the axial ligands is quite constant (0.1-0.3 e on imidazole and -0.01 to -0.25 e on the methyl group). Consequently, the major difference in the charge density between the various complexes (with a total charge ranging from -1 to +2) is found in the ring system: The total charge in the porphyrin ring varies between -1.39 and -0.32 e and the corrin charge

varies between -0.54 and +0.64 e.

In Tables 7 and 8 we also include the spin density on the metal ion for the various complexes. In all open-shell complexes, the spin density is close to 1, indicating that almost all unpaired spin density is located on the metal ion, although there is a significant spin density also on the methyl groups ( $\sim -0.15$  e). However, the two  $\text{Co}^{\text{II}}\text{MeIm}$  complexes differ radically from the other complexes: In these, there is essentially no spin density on Co and Me. Instead, all the spin is found in the porphine or corrin rings. Apparently, it is more favourable in these complexes to form a Por/Cor radical and  $\text{Co}^{\text{III}}$  ion, which is  $d^6$  with an empty  $d_{z^2}$  orbital, and therefore forms better bonds with the strong methyl ligand, whereas with the two weaker imidazole ligands, the  $d^7$  state is more stable.

Table 9 shows the corresponding results for the four-coordinate  $\text{M}^{\text{I/II}}\text{Cor/Por}$  complexes. They are similar to those of the six-coordinate complexes, with a metal charge of 0.50-0.74 e and a variable ring charge. However, the  $\text{M}^{\text{I}}$  complexes show some interesting features: The  $\text{Fe}^{\text{I}}$  complexes are doublets with a spin population close to 2 on Fe (1.9-2.0) and with one unpaired electron delocalised in the ring system. Thus the iron complexes are triplet  $\text{Fe}^{\text{II}}$ , antiferromagnetically coupled to a porphine or corrin radical. Apparently, the reduction potential of the  $\text{Fe}^{\text{II}}/\text{Fe}^{\text{I}}$  couple is lower than the energy needed to form a ring

radical. As we saw above, the same is true also for the  $\text{Co}^{\text{I}}$  complexes: Their lowest electronic states are open-shell singlets, formed from doublet  $\text{Co}^{\text{II}}$ , antiferromagnetically coupled to a ring radical. However, the closed-shell singlets are only 4-18 kJ/mole higher in energy.

### *Reduction potential*

Another possible reason for the selection of certain combinations of ions and rings is differences in the reduction potential between the two metal ions and the two ring systems. In aqueous solution, iron is more easily oxidised than cobalt. For example, the  $\text{Co}^{0/\text{II}}$  potential (-0.28 V) is less negative than the corresponding  $\text{Fe}^{0/\text{II}}$  potential (-0.44 V). Similarly, the  $\text{Co}^{\text{II}/\text{III}}$  potential (+1.82 V) is more positive than the  $\text{Fe}^{\text{II}/\text{III}}$  potential (+0.77 V; all potentials are relative to the standard hydrogen electrode).<sup>[48]</sup> Therefore, we have studied the reduction potentials of the various complexes in the present investigation.

When calculating reduction potentials, solvation energies are as important as the electronic energies. These have been estimated by the COSMO continuum model, using three different values of the dielectric constant ( $\epsilon$ ): 1 (vacuum), 4, and 80. The last value is close to what is found in bulk water solution, whereas the whole series gives an impression of what effects can be expected inside a protein, where the effective dielectric constant has been estimated to be 2-16.

[53,54] The results of these calculations for the Im<sub>2</sub> and Im-Me complexes in their low-spin ground states are shown in Table 10.

Two clear trends can be seen from these results. First, a cobalt ion has a 0.2-0.5 V *lower* reduction potential than the corresponding iron complex. This represents the intrinsic difference between iron and cobalt with these ligands. The sign of the difference is somewhat unexpected, because it indicates that Co<sup>2+</sup> is more easily oxidised than Fe<sup>2+</sup> although the contrary is found for the ions in aqueous solution.<sup>[48]</sup> However, this is an effect of the tetra-pyrrole rings; for the isolated and hydrated ions, similar calculations indicate that iron is the most easily oxidised ion (for example, the M(H<sub>2</sub>O)<sub>6</sub> complexes studied with  $\epsilon = 80$  reproduce exactly the experimental 0.99-V difference between Co<sup>II/III</sup> and Fe<sup>II/III</sup>).<sup>[48]</sup> Thus, the ring systems selectively stabilises the Co<sup>III</sup> state compared to Fe<sup>III</sup>.

Second, it can be seen that porphine gives rise to a lower reduction potential than does corrin. The reason for this is that the double negative charge of the porphine ring stabilises (solvates) the higher charge of the oxidised state better than the single negative charge of corrin. The same argument also explains why the Im-Me complexes have lower reduction potentials than the Im<sub>2</sub> complexes.

We also see that the difference in reduction potential between porphine and corrin depends strongly on  $\epsilon$ , but not so

much on the metal. The reason for this is also the differing charge of the two ring systems, leading to different total charges of the complexes. The solvation energy depends strongly on the total charge of the complex (cf. the simple Born model, in which the solvation energy is proportional to the square of the total charge). This explains why the reduction potential of all complexes decreases with (the total charge increases during oxidation) except for the MPorImMe complexes, in which the total charge decreases during oxidation.

Together, the result of these two effects is that the two native combinations FePor and CoCor have quite similar reduction potentials (especially in water). The two other combinations have either higher (CoPor) or lower (FeCor) potentials, but the difference is not very large in water (0.2-0.5 V).

The reduction potential of the FePorIm<sub>2</sub> complex ranges from -0.7 in water to +0.4 V in vacuum. This is in reasonable accordance with the measured reduction potential of cytochromes, which range between -0.4 and +0.5 V.<sup>[5,49]</sup> The corresponding CoCorIm<sub>2</sub> model has a potential that is more sensitive to and in general somewhat higher (-0.7 to +3.2 V). Thus, the reduction potentials give no clear reason why cobalt or corrin are not employed for biological electron transfer. Likewise, for the Im-Me complexes, the reduction potentials of CoCorMeIm and FePorMeIm partly overlap,

although that of the former complex is in general higher.

An important reason for using corrin for heterolytic Co-C bond cleavage may be to make the the  $\text{Co}^{\text{I}}$  state accessible; this state would be anticipated to be unfavourable in a porphyrin ring, compared with species of higher oxidation state, due to increased inter-electron repulsion in the ligand field. Thus, it has been suggested that the  $\text{Co}(\text{I})$  state is not accessible in  $\text{CoPor}$  systems<sup>[10]</sup> and it has also been observed that  $\text{FeCor}$  can be oxidised to  $\text{Fe}(\text{I})$ , but it cannot be methylated.<sup>[11]</sup> Therefore, we have also studied the reduction potentials of the four-coordinate  $\text{M}^{\text{I}}$  and  $\text{M}^{\text{II}}$  complexes without any axial ligands. These results are also included in Table 10.

Interestingly, the reduction potentials of the four-coordinate complexes are similar to those of the six-coordinate complexes. Cobalt gives rise to slightly lower reduction potentials than does iron (0-0.2 V), but the difference is smaller and reversed at the highest dielectric constant, and there are large effects of the ring system, especially at low values of . However, the reduction potential of  $\text{FePor}$  is always lower than that of  $\text{CoCor}$ . The difference is largest at low values of , but even in water solution, the difference is predicted to be 0.4 V. Thus, it should be appreciably harder to form  $\text{Fe}^{\text{I}}\text{Por}$  than  $\text{Co}^{\text{I}}\text{Cor}$ . The same applies to  $\text{CoPor}$ , which is quite similar to  $\text{FePor}$ , confirming the suggestion that the  $\text{Co}(\text{I})$  state is not



accessible in CoPor.<sup>[10]</sup> Yet, the FeCoR complex is predicted to be more easily reduced than the native CoCoR complex.

### *Reorganisation energies*

We will now turn to some functional aspects of the various combinations of ions and ring systems. We have concentrated on one typical reaction for each of the two native combinations, i.e. the Co-C bond dissociation reaction, as a typical reaction for CoCoR in coenzyme B<sub>12</sub>, and electron transfer, as a typical reaction for FePor in the cytochromes, although we recognise that haem proteins have a number of other functions.

Electron transfer is a special reaction, in that its only effect is to move an electron from one site to another. According to the semiclassical Marcus theory,<sup>[50]</sup> the rate of electron transfer depends on three terms, the reduction potential (which we have already studied), the electronic coupling element (which is mainly a function of the distance between the donor and the acceptor sites), and the reorganisation energy ( $\lambda$ ). The latter term measures how much the geometry of the donor and acceptor sites changes during the redox process. It is normally divided into two contributions, the inner- and outer-sphere reorganisation energy ( $\lambda_i$  and  $\lambda_o$ ), depending on what atoms are relaxed. For a metal-containing protein, the inner-sphere reorganisation energy is associated with the structural change of the first

coordination sphere, whereas the outer-sphere reorganisation energy involves structural changes of the remaining protein as well as the solvent.

We have calculated the inner-sphere reorganisation energy for the four combinations of ions and ring systems. It is calculated as the energy difference of the reduced complex at its optimum geometry and at the optimum geometry of the oxidised complex ( $_{red}$ ) or vice versa ( $_{ox}$ ).<sup>[51]</sup> For a self-exchange reaction,  $\epsilon_i = \epsilon_{red} + \epsilon_{ox}$ . This approach has been successfully applied to several proteins,<sup>[52-55]</sup> in particular for cytochrome models with various sets of axial ligands.<sup>[37]</sup>

The reorganisation energies of the  $Im_2$  complexes (models of several *b*- and *c*-type cytochromes) are shown in Table 11. They show that the two iron complexes give almost the same reorganisation energy, 8-9 kJ/mole. Therefore, iron corrin would form an equally excellent electron-transfer site as iron porphyrin, but at higher potentials. It has been shown<sup>[37]</sup> that the LS state of the site is essential for the low reorganisation energy, but we have seen that corrin stabilises the LS of iron even better than porphyrin. Therefore, the reorganisation energies do not give any clue why Nature has selected porphyrins rather than corrins in the cytochromes.

However, for the two cobalt complexes in Table 11, the reorganisation energies are very large, 179-197 kJ/mole. The reason for these high values is the large change in the Co-

$N_{Im}$  distances (owing to the occupied  $d_{z^2}$  orbital for  $Co^{II}$ ; cf. Table 5). The iron systems have similar axial bond lengths (within 4 pm) for both oxidation states, owing to the fact that the  $d_{z^2}$  and  $d_{x^2-y^2}$  orbitals are empty in both oxidation states.

This gives a direct explanation why cobalt (at least the  $Co^{II/III}$  couple in octahedral geometry) has not been used for electron transfer. A reorganisation energy of 179–197 kJ/mole is much larger than what is obtained for native electron-transfer sites (4–40 kJ/mole<sup>[37]</sup>). We conclude that evolutionary design of tetrapyrrole electron transfer systems may involve either corrins or porphyrins, but not  $Co^{II/III}$ .

#### *Bond dissociation energies*

As a typical reaction for CoCor in coenzyme  $B_{12}$ , we will study the homolytic Co-C bond dissociation energy (BDE), i.e. the energy of the reaction



The experimental BDE of methylcobalamin is  $155 \pm 12$  kJ/mol.<sup>[56,57]</sup> The Co-C bond strength of various cobalamin models have been calculated with the B3LYP density functional by three groups.<sup>[24,41,42]</sup> They obtained BDEs of 91–117 kJ/mole using the same type of model as we use (CoCorImMe), i.e. far from the experimental value. Recently, we have shown that this is a shortcoming of the B3LYP method.<sup>[47]</sup> Other density functionals (e.g. BP86) and second-order Møller-Plesset perturbation

theory (MP2) give result close to the experimental value (148-160 kJ/mole). Therefore, we calculate the Co-C BDE at the BP86 level of theory in this paper.

The calculated Co-C BDEs for the four combinations of ions and ligands are shown in Table 12. They are obtained for the lowest spin state for all reactants, i.e. the LS state for all cobalt complexes and for the six-coordinate iron complexes, but the IS state of the five-coordinate iron complexes (c.f. Table 2). It can be seen that the BDEs are quite similar, varying from 147 kJ/mole for the FePor complex to 159 kJ/mole for the CoCor model. Solvation effects are small (1-7 kJ/mole) and do not change the order between the various complexes, as can also be seen in Table 12.

Thus, the combination employed in nature has the *highest* Co-C BDE. This may at first seem a bit strange, because the Co-C bond is broken during the biochemical reaction. However, as Pratt has argued, the Co-C bond must be stable against hydrolysis.<sup>[11]</sup> In fact, he attributes the strong Co-C bond to the low 3d to 4s/4p promotion energy of Co<sup>II</sup>, which gives strong covalent bonds with carbon.<sup>[11]</sup>

This has led us to study the hydrolysis of the six-coordinate Im-Me complexes, i.e. the reaction:<sup>[11]</sup>

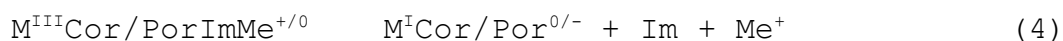


The calculated reaction energies for the four combinations of ions and ring systems (using the LS ground state for all metal complexes) are shown in Table 13. They indicate that

all methyl complexes are unstable towards hydrolysis by 71-122 kJ/mole. However, the cobalt complexes are much more stable (by 33-48 kJ/mole) than the corresponding iron complexes. This gives a strong reason why cobalt is selected, rather than iron, as a methyl donor or radical carrier.

#### *Methyl-transfer reactions*

Our results also give us the opportunity to study the other type of cobalamin reaction, i.e. the heterolytic cleavage of the  $\text{Co}^{\text{III}}\text{-C}$  bond, giving a four-coordinate  $\text{Co}^{\text{I}}$  complex and formally a  $\text{CH}_3^+$  cation, which is transferred to a nucleophilic substrate, e.g. homocysteine. This reaction can either be studied as a heterolytic Co-C BDE:



or with a substrate included, e.g.  $\text{CH}_3\text{S}^-$  (as a model of homocysteine in a methionine synthetase-like reaction):



Both reactions give the same relative result, although the absolute values are shifted by a large constant. The results for the reaction in Eqn. (5) are gathered in Table 14.

It can be seen that the reaction energy varies much with the dielectric constant, as can be expected for a reaction altering the charges of the reactants. At a low dielectric constant, the corrin complexes give the most negative reaction energies, whereas in water solution, all four complexes are predicted to give similar reaction energies

(within 12 kJ/mole). Therefore, the homolytic methyl-transfer reaction does not provide any clear explanation why the cobalamins were selected in Nature. On the contrary, iron gives a 8-19 kJ/mole lower reaction energy than cobalt.

#### *Concluding remarks*

In this paper, we have studied how the properties of iron and cobalt porphyrins and corrins differ in various aspects. The results have given us several clues how the seemingly similar structures of iron porphyrin and cobalt corrin give rise to their different functions.

First, we have seen that the thermodynamic stability favours the two native combinations of ions and ring systems by 8-24 kJ/mole over the non-native combinations for all complexes, except the Im-Me  $M^{II}$  complexes. Thus, there is some intrinsic thermodynamic reason to choose the native combinations.

Second, and probably most important, the central cavity of the corrin ring is smaller than that of the porphine ring. Therefore, corrin favours the low-spin states of  $Co^{III}$  and  $Co^{II}$ , and even the four-coordinate low-spin  $Co^I$  (formally) ion fits well into the corrin ring. Thus, CoCor is always low spin and all reactants and intermediates in the cobalamin reaction cycles involve small strain in the ring system. On the other hand, the cavity in porphine is too large for the low-spin cobalt and iron ions. Instead, it

seems to be more appropriate for the intermediate-spin states. Consequently, intermediate and high-spin states are available for the FePor complexes, and they are important for many of the reactions of haem proteins, e.g. in the binding and activation of O<sub>2</sub>.

Third, Co<sup>III</sup> in aqueous solution is more easily reduced than iron. However, in the tetra-pyrrole rings, this tendency have been reversed, so that cobalt consistently gives 0.1-0.3 eV lower potentials than iron. There are also pronounced differences in the reduction potentials of the corrin and porphine rings, in that the former gives higher potentials. These are mainly caused by the differing charge of the ring system and therefore strongly depends on solvation effects. As an effect of these two opposing tendencies, the native FePor and CoCor combinations often give quite similar reduction potentials at high dielectric constants, but the latter has a higher potential in most solvents. In particular, four-coordinate Co<sup>I</sup>Cor is more easily formed than Fe<sup>I</sup>Por, making it accessible in corrin chemistry.

Fourth, the octahedral Fe<sup>II/III</sup>Por/CorIm<sub>2</sub> complexes have much lower inner-sphere reorganisation energies (8-9 kJ/mole) than the corresponding Co<sup>II/III</sup> complexes (179-197 kJ/mole). The reason for this is the occupation of the *d*<sub>22</sub> orbital in low-spin Co<sup>II</sup> (*d*<sup>7</sup>), leading to a large difference in the distances to the axial ligands in the two oxidation states. Therefore, the Co<sup>II/III</sup> couple is useless for electron-transfer

reactions, whereas the octahedral Fe<sup>II/III</sup> complexes (d<sup>5/6</sup>) form excellent electron carriers, also compared with other metal sites.<sup>[37]</sup>

Finally, CoCorImMe has the largest homolytic Co-C BDE of the studied complexes, even if the variation is only 12 kJ/mole. This is compensated by the largest resistance towards hydrolysis. The cobalt complexes are appreciably more stable towards hydrolysis than the iron complexes (by ~40 kJ/mole). This may explain why cobalamins are employed in the nature for organometallic reactions.

In conclusion, we have identified several good reasons why iron is associated with porphine in nature, whereas cobalt is associated with corrin, and also why the FePor complexes are used for electron transfer and oxygen activation, whereas CoCor are involved in organometallic Co-C reactions (methyl transfer and radical formation).

## **Methods**

### *Models*

We have included the full porphine (Por) or corrin (Cor) ring systems in our models, because this is the basic entity of the coenzymes, and loss of equatorial conjugation energy may have a drastic effect on the electron structure. All side chains on the rings have been replaced by hydrogen atoms in the models to allow for a comparison of the fundamental chemistry of the corrin and porphine rings. Earlier



calibrations have shown that they have a small influence on the structure and properties of the ring system.<sup>[58]</sup> We have studied five types of models, differing in the axial ligands: Three are octahedral with two axial ligands, either two imidazole groups ( $\text{Im}_2$ ), one Im and one methyl group (Me), or one Im and one hydroxide ion. In addition, we studied five-coordinate complexes with an Im ligand and four-coordinate complexes without any axial ligands. The following oxidation states have been studied:  $\text{M}^{\text{II}}$  and  $\text{M}^{\text{III}}$  (M denotes the metal, Co or Fe) for the complexes with  $\text{Im}_2$  and Im-Me,  $\text{M}^{\text{III}}$  for the Im-OH complexes,  $\text{M}^{\text{II}}$  for the five-coordinate complexes, and  $\text{M}^{\text{I}}$  and  $\text{M}^{\text{II}}$  for the four-coordinate complexes. All systems were optimised in the lowest (ground) spin state, according to experiments or calculations. For the Im-Me, Im, and four-coordinate complexes, we also optimised the high and intermediate-spin states. Some of the native combinations of ions and ring systems ( $\text{Fe}^{\text{II/III}}\text{PorIm}_2$ ,  $\text{Co}^{\text{III}}\text{CorImMe}$ ,  $\text{Fe}^{\text{II/III}}\text{PorIm}$ ,  $\text{Co}^{\text{II}}\text{CorIm}$ ,  $\text{Fe}^{\text{II}}\text{Por}$ ,  $\text{Co}^{\text{II}}\text{Por}$ , and  $\text{Co}^{\text{I}}\text{Cor}$ ) have been studied before by theoretical methods,<sup>[16,24-42]</sup> but only for the latter three has the aim been to compare the properties of the ions and rings.<sup>[16]</sup>

### *Computational Details*

All calculations were performed with the Becke three-parameter hybrid functional B3LYP, which combines some exact Hartree-Fock exchange with the local spin-density correlation

functional of Vosko-Wilk-Nusair and the non-local Lee-Yang-Parr correlation functionals.<sup>[59]</sup> B3LYP is widely recognised as one of the most accurate density functional methods, in general terms for structures, energies, and frequencies.<sup>[60,61]</sup> However, for the Co-C bond dissociation energy, calibration calculations have shown that B3LYP gives very poor results.<sup>[62]</sup> Therefore, we used the density functional Becke-Perdew 86 (BP) method for these (single-point) energies.<sup>[63,64]</sup>

The calculations were carried out with the Turbomole program, versions 5.3 and 5.5.<sup>[65]</sup> The geometry optimisations were run using the 6-31G\* basis set for all atoms except the metal. This basis set assigns one set of polarisation functions to all non-hydrogen atoms. For cobalt and iron, we used the double- basis set of Schäfer *et al.* (contraction scheme *14s11p6d1f / 8s7p4d1f*),<sup>[66]</sup> augmented with two *p*, one *d*, and one *f* functions (with exponents 0.141308, 0.043402, 0.1357, and 1.62 for Co and 0.134915, 0.41843, 0.1244, and 1.339 for Fe). Only the pure five *d* and seven *f*-type functions were used. We applied the default (m3) grid size of Turbomole, and all optimisations were carried out in redundant internal coordinates. Fully unrestricted calculations were performed for the open-shell systems. We made use of the default convergence criteria, which imply self-consistency down to  $10^{-6}$  Hartree (2.6 J/mol) for the energy and  $10^{-3}$  a.u. (0.053 pm or 0.057°) for the internal degrees of freedom.

After optimisation, accurate energies for most of the structures were calculated with the large triple-6-311+G(2d,2p) basis set, which includes diffuse functions on heavy atoms and polarisation functions on all atoms. The basis sets of the metals were augmented by one *s* function (exponents Co: 0.0145941 and Fe: 0.01377232) and the *f* function was replaced by two new functions (exponents Co: 2.8 and 0.8 and Fe: 2.5 and 0.8).

### *Solvation energies*

Normal quantum chemical calculations are performed in vacuum, whereas most reactions take place in water solution or in proteins. In order to correct for this discrepancy, we have calculated solvation energies for most complexes using the continuum conductor-like screening model (COSMO),<sup>[67]</sup> as implemented in Turbomole 5.5. In this method, the solute molecule forms a cavity within a dielectric continuum characterised by a dielectric constant,  $\epsilon$ . The charge distribution of the solute polarises the dielectric medium and the response of the medium is described by the generation of screening charges on the surface of the cavity.

These calculations were performed with default values for all parameters (implying a water-like probe molecule) and a dielectric constant of 4 and 80, to model pure water and to get a feeling of possible effects in a protein (where the effective dielectric constant is normally estimated to 2-16).

[<sup>68,69</sup>] For the generation of the cavity, a set of atomic radii have to be defined. We used the optimised COSMO radii in Turbomole (H: 1.30 Å, C: 2.00 Å, N: 1.83 Å, O: 1.72 Å, Fe: 2.00 Å, Co: 2.00 Å).

Reduction potentials were estimated from these energies in a solvent according to Eqn. 6:

$$E^0 = E(\text{ox}) - E(\text{red}) - 4.43 \quad (6)$$

where the factor of 4.43 eV represents the potential of the standard hydrogen electrode.<sup>[70]</sup>

*Acknowledgements.* This investigation has been supported by grants from the Swedish research council (VR) and by computer resources of Lunarc at Lund university.

## References

- [1] M. Sono, M. R. Roach, E. D. Coulter, J. H. Dawson, *Chem. Rev.* **1996**, *96*, 2841.
- [2] J. P. Glusker, *Vitamins and Hormons* **1995**, *50*, 1.
- [3] M. L. Ludwig, R. G. Matthews, *Annu. Rev. Biochem.* **1997**, *66*, 269.
- [4] R. Banerjee, *Chemistry and Biology* **1997**, *4*, 175.
- [5] J. J. R. Frausto da Silva, R. J. P. Williams, *The biological chemistry of the elements*, Clarendon Press, Oxford, **1994**, p. 10.
- [6] M. D. Wirt, I. Sagi, E. Chen, S. M. Frisbie, R. Lee, M. R. Chance, *J. Am. Chem. Soc.* **1991**, *113*, 5299.

- [7] W. R. Scheidt, C. A. Reed, *Chem. Rev.* **1981**, *81*, 543.
- [8] R. K. Suko, L. Poppe, J. Rétey, R. G. Finke, *Bioorganic Chemistry* **1999**, *27*, 451.
- [9] M. D. Wirt, I. Sagi, M. R. Chance, *Biophys. J.* **1992**, *63*, 412.
- [10] W. Kaim, B. Schwederski, *Bioinorganic chemistry: Inorganic elements in the chemistry of life.*, John Wiley & Sons, Chichester, **1994**, p. 42.
- [11] J. M. Pratt, *Pure & Applied Chemistry* **1993**, *65*, 1513.
- [12] A. M. Stolzenberg, M. T. Stershic, *J. Am. Chem. Soc.* **1988**, *110*, 6391.
- [13] J. J. R. Frausto da Silva, R. J. P. Williams, *The biological chemistry of the elements*, Clarendon Press, Oxford, **1994**, p. 403.
- [14] M. K. Geno, J. Halpern, *J. Am. Chem. Soc.* **1987**, *109*, 1238.
- [15] S. J. Lippard, J. M. Berg, *Principles of bioinorganic chemistry*, University science books, Mill Valley, CA, **1994**, p. 343.
- [16] C. Rovira, K. Kunc, J. Hutter, M. Parrinello, *Inorg. Chem.* **2001**, *40*, 11.
- [17] R. J. P. Williams, *J. Mol. Catal.* **1985**, *30*, 1.
- [18] Y. Murakami, Y. Aoyama, K. Tokunaga, *J. Am. Chem. Soc.* **1980**, *102*, 6736.
- [19] J. M. Pratt in *B<sub>12</sub>*, vols. 1-2, (ed.: D. Dolphin), Wiley, New York, **1982**, p. 325.

- [20] E. Scheuring, R. Padmakumar, R. Banerjee, M. R. Chance, *J. Am. Chem. Soc.* **1997**, *119*, 12192.
- [21] S. Dong, R. Padmakumar, R. Banerjee, T. G. Spiro, *J. Am. Chem. Soc.* **1996**, *118*, 9182.
- [22] S. Dong, R. Padmakumar, R. Banerjee, T. G. Spiro, *J. Am. Chem. Soc.* **1999**, *121*, 7063.
- [23] J. M. Sirovatka, A. K. Rappé, R. G. Finke, *Inorg. Chim. Acta* **2000**, *300-302*, 545.
- [24] K. P. Jensen, U. Ryde, *J. Mol. Struct. (Theochem)* **2002**, *585*, 239.
- [25] M.-M. Rohmer, *Chem. Phys. Lett.* **1985**, *116*, 44.
- [26] W. D. Edwards, B. Weiner, M. C. Zerner, *J. Am. Chem. Soc.* **1986**, *108*, 2196.
- [27] Y.-K. Choe, T. Hashimoto, H. Nakano, K. Hirao, *Chem. Phys. Lett.* **1998**, *295*, 380.
- [28] Y.-K. Choe, T. Nakajima, K. Hirao, R. Lindh, *J. Chem. Phys.* **1999**, *111*, 3837.
- [29] T. G. Spiro, P. M. Kozlowski, M. Z. Zgierski, *J. Raman Spectr.* **1998**, *29*, 869.
- [30] P. M. Kozlowski, T. G. Spiro, A. Bérces, M. Z. Zgierski, *J. Phys. Chem. B* **1998**, *102*, 2603.
- [31] Y. Seno, N. Kameda, J. Otsuka, *J. Chem. Phys.* **1980**, *72*, 6048.
- [32] S. Obara, H. Kashiwagi, *J. Chem. Phys.* **1982**, *77*, 3155.
- [33] S. Yamamoto, J. Teraoka, H. Kashiwagi, *J. Chem. Phys.* **1988**, *88*, 303.

- [34] N. Matsuzawa, M. Ata, D. A. Dixon, *J. Phys. Chem.* **1995**, *99*, 7698.
- [35] C. Rovira, K. Kunc, J. Hutter, P. Ballone, M. Parinello, *J. Phys. Chem. A* **1997**, *101*, 8914.
- [36] E. Sigfridsson, U. Ryde, *J. Biol. Inorg. Chem.* **1999**, *4*, 99.
- [37] E. Sigfridsson, M. H. M. Olsson, U. Ryde, *J. Phys. Chem. B* **2001**, *105*, 5546.
- [38] T. Andruniow, M. Z. Zgierski, P. M. Kozlowski, *J. Phys. Chem. B* **2000**, *104*, 10921.
- [39] T. Andruniow, M. Z. Zgierski, P. M. Kozlowski, *Chem. Phys. Lett.* **2000**, *331*, 509.
- [40] K. P. Jensen, S. P. A. Sauer, T. Liljefors, P.-O. Norrby, *Organometallics* **2001**, *20*, 550.
- [41] N. Dölker, F. Maseras, A. Lledos, *J. Phys. Chem. B* **2001**, *105*, 7564.
- [42] T. Andruniow, M. Z. Zgierski, P. M. Kozlowski, *J. Am. Chem. Soc.* **2001**, *123*, 2679.
- [43] M. L. Ludwig, R. G. Matthews, *Annu. Rev. Biochem.* **1997**, *66*, 269.
- [44] R. H. Holm, P. Kennepohl, E. I. Solomon, *Chem. Rev.* **1996**, *96*, 2239.
- [45] A. Eschenmoser, *Angew. Chem. Int. Ed.* **1988**, *27*, 5.
- [46] T. S. Rush, III, P. M. Kozlowski, C. A. Piffat, R. Kumble, M. Z. Zgierski, T. G. Spiro, *J. Phys. Chem. B* **2000**, *104*, 5020.

- [47] J. L Hoard, *Science* **1971**, *174*, 1295.
- [48] J. G. Stark, H. G. Wallace, *Chemistry Data Book*, John Murray, London, **1982**.
- [49] H.-X. Zhou, *J. Biol. Inorg. Chem.* **1997**, *2*, 109.
- [50] R. A. Marcus, N. Sutin, *Biochim. Biophys. Acta* **1985**, *811*, 265.
- [51] A. Klimkans, S. Larsson, *Chem. Phys. Lett.* **1994**, *189*, 25.
- [52] M. H. M. Olsson, U. Ryde, B. O. Roos, *Prot. Sci.* **1998**, *7*, 2659.
- [53] U. Ryde, M. H. M. Olsson, *Intern. J. Quant. Chem.* **2001**, *81*, 335.
- [54] E. Sigfridsson, M. H. M. Olsson, U. Ryde, *Inorg. Chem.* **2001**, *40*, 2509.
- [55] M. H. M. Olsson, U. Ryde, *J. Am. Chem. Soc.* **2001**, *123*, 7866.
- [56] B. D. Martin, R. G. Finke, *J. Am. Chem. Soc.* **1990**, *112*, 2419.
- [57] B. D. Martin, R. G. Finke, *J. Am. Chem. Soc.* **1992**, *114*, 585.
- [58] E. Sigfridsson, U. Ryde, *J. Biol. Inorg. Chem.* **2003**, in press; DOI: 10.1007/s00775-002-0413-8.
- [59] R. H. Hertwig, W. Koch, *Chem. Phys. Lett.* **1997**, *268*, 345.
- [60] C. W. Bauschlicher, *Chem. Phys. Lett.* **1995**, *246*, 40.
- [61] P. E. M. Siegbahn, M. R. A. Blomberg, *Chem. Rev.* **2000**,



100, 421.

- [62] K. P. Jensen, U. Ryde, *J. Phys. Chem. B* **2003**, submitted.
- [63] A. D. Becke, *Phys. Rev. A* **1988**, 38, 3089.
- [64] J. P. Perdew, *Phys. Rev. B* **1986**, 33, 8822.
- [65] R. Alrichs, M. Bär, M. Häser, H. Horn, C. Kölmel, *Chem. Phys. Lett.* **1989**, 162, 165.
- [66] A. Schäfer, H. Horn, R. Ahlrichs, *J. Chem. Phys.* **1992**, 97, 2571.
- [67] A. Klamt, J. Schüürmann, *J. Chem. Soc. Perkin Trans.* **1993**, 2, 799.
- [68] K. A. Sharp, *Annu. Rev. Biophys. Biophys. Chem.* **1990**, 19, 301.
- [69] B. Honig, *Science* **1995**, 268, 1144.
- [70] H. Reiss, A. Heller, *J. Phys. Chem.* **1985**, 89, 4207.

## Legends to the figures

**Figure 1.** The porphyrin (left) and corrin (right) ring systems.

**Figure 2.** Optimised structures of the studied CoCor and FePor complexes.

**Figure 3.** The  $M(\text{NH}(\text{CH})_3\text{NH})_2$  (left) and  $M(\text{NH}(\text{CH})_3\text{NH})(\text{CH}_2\text{NH}(\text{CH})_2\text{NHCH}_2)$  (right) models with removed ring strain.

**Table 1.** The energy difference (kJ/mole) between the low-spin and intermediate-spin states of the MCor/PorImMe complexes.

	<b>Fe<sup>II</sup></b>	<b>Co<sup>II</sup></b>	<b>Fe<sup>III</sup></b>	<b>Co<sup>III</sup></b>
Porphyrin	39	78	46	82
Corrin	<b>35</b>	- <sup>a</sup>	92	139

<sup>a</sup> No stable octahedral minimum for the quartet state.

**Table 2.** The energy difference (kJ/mole) between the various spin states of the five-coordinate M<sup>II</sup>Cor/PorIm complexes and the four-coordinate M<sup>I</sup>Cor/Por complexes.

Spin state	LS	IS	HS
Fe <sup>II</sup> PorIm	28	0	4
Fe <sup>II</sup> CorIm	21	0	29
Co <sup>II</sup> PorIm	0	21	
Co <sup>II</sup> CorIm	0	58	
Fe <sup>I</sup> Por	0	13	28
Fe <sup>I</sup> Cor	0	31	112
Co <sup>I</sup> Por	0 (-18 <sup>a</sup> )	4	
Co <sup>I</sup> Cor	0 (-4 <sup>a</sup> )	75	

<sup>a</sup> Open-shell singlet state.

**Table 3.** Thermodynamic stabilities, Eqn. (1), of complexes with various axial ligands and oxidation states, calculated at different values of the dielectric constant ( ).

Axial ligands	Oxidation state	= 1	= 4	= 80
Im <sub>2</sub>	+II	12.2	10.7	9.6
	+III	7.8	8.0	8.1
Im-Me	+II	-13.2	-12.5	-11.4
	+III	16.8	17.0	17.1
Im-OH	+III	18.6	15.9	14.1
Im	+II	14.2	14.3	14.4
-	+I	19.5	20.8	21.1
-	+II	21.4	22.6	23.9

**Table 4.** Metal-ligand bond distances (pm) of the optimised MCor/PorImMe complexes in their low-spin ground states.

<b>Structure</b>	<b>M-C</b>	<b>M-N<sub>Im</sub></b>	<b>M-N<sub>eq,av</sub></b>
Fe <sup>II</sup> PorImMe <sup>-</sup>	200.5	222.8	201.5
Fe <sup>II</sup> CorImMe <sup>0</sup>	201.0	226.0	192.1
Co <sup>II</sup> PorImMe <sup>-1</sup>	195.2	220.4	202.0
Co <sup>II</sup> CorImMe <sup>0</sup>	195.9	225.2	192.8
Fe <sup>III</sup> PorImMe <sup>0</sup>	198.9	224.9	201.8
Fe <sup>III</sup> CorImMe <sup>+</sup>	199.6	229.0	193.3
Co <sup>III</sup> PorImMe <sup>0</sup>	195.7	221.2	200.6
Co <sup>III</sup> CorImMe <sup>+</sup>	196.6	225.0	192.0

**Table 5.** Metal-ligand bond distances (pm) of the optimised MCor/PorIm<sub>2</sub> complexes in their low-spin ground states.

<b>Structure</b>	<b>M-N<sub>Im1</sub></b>	<b>M-N<sub>Im2</sub></b>	<b>M-N<sub>eq,av</sub></b>
Fe <sup>II</sup> PorIm <sub>2</sub> <sup>-</sup>	202.4	204.5	204.5
Fe <sup>II</sup> CorIm <sub>2</sub> <sup>0</sup>	206.0	209.1	193.5
Co <sup>II</sup> PorIm <sub>2</sub> <sup>-1</sup>	240.0	240.1	201.2
Co <sup>II</sup> CorIm <sub>2</sub> <sup>0</sup>	247.3	251.0	192.1
Fe <sup>III</sup> PorIm <sub>2</sub> <sup>0</sup>	201.2	202.6	202.6
Fe <sup>III</sup> CorIm <sub>2</sub> <sup>+</sup>	204.7	204.8	193.5
Co <sup>III</sup> PorIm <sub>2</sub> <sup>0</sup>	197.9	198.1	200.6
Co <sup>III</sup> CorIm <sub>2</sub> <sup>+</sup>	199.5	201.6	192.5

**Table 6.** Calculated metal-ligand distances (pm) for four types of complexes with the ligand  $L = (\text{NH}(\text{CH})_3\text{NH})_2$ , simulating a broken ring system. The  $\text{M-N}_{\text{eq}}$  distances for the corresponding porphyrin and corrin complexes are also included for comparison.

<b>Structure</b>	<b>M-N<sub>Im1</sub></b>	<b>M-N<sub>Im2</sub></b>	<b>M-N<sub>eq, av</sub></b>	<b>Cor</b>	<b>Por</b>
$\text{Fe}^{\text{II}}L_2\text{Im}_2$	205.4	205.4	198.8	193.5	204.5
$\text{Fe}^{\text{III}}L_2\text{Im}_2$	204.7	204.7	194.0	193.5	202.6
$\text{Co}^{\text{II}}L_2\text{Im}_2$	250.4	254.6	194.5	192.1	201.2
$\text{Co}^{\text{III}}L_2\text{Im}_2$	199.3	199.3	193.9	192.5	200.6
$\text{Co}^{\text{III}}L_2\text{ImMe}$	227.4	195.7	193.6	192.0	200.6
$\text{Co}^{\text{II}}L_2\text{Im}$	228.5	-	195.3	192.1	200.6
$\text{Co}^{\text{I}}L_2$	-	-	190.4	188.6	198.8



**Table 7.** Mulliken charges, spin density, and 3d population on some atoms and groups of atoms in the MCor/PorImMe complexes.

Compound	M	charge on				4N <sub>eq</sub>	spin on M	M 3d population
		CH <sub>3</sub>	Im	Ring				
Fe <sup>II</sup> PorImMe <sup>-</sup>	0.57	-0.27	0.08	-1.38	-2.08	-	6.57	
Fe <sup>II</sup> CorImMe	0.55	-0.24	0.10	-0.41	-1.78	-	6.62	
Co <sup>II</sup> PorImMe <sup>-</sup>	0.57	-0.09	0.12	-1.60	-2.18	0.00	7.42	
Co <sup>II</sup> CorImMe	0.54	-0.08	0.13	-0.59	-1.87	0.01	7.46	
Fe <sup>III</sup> PorImMe	0.66	-0.07	0.15	-0.74	-2.19	1.19	6.40	
Fe <sup>III</sup> CorImMe <sup>+</sup>	0.64	-0.05	0.16	0.25	-1.91	1.16	6.44	
Co <sup>III</sup> PorImMe	0.56	-0.03	0.16	-0.69	-2.13	-	7.43	
Co <sup>III</sup> CorImMe <sup>+</sup>	0.54	-0.01	0.17	0.30	-1.85	-	7.47	

**Table 8.** Mulliken charges, spin density, and 3d population on some atoms and groups of atoms the MCor/PorIm<sub>2</sub> complexes.

Compound	M	charge on				4N <sub>eq</sub>	spin on M	M 3d population
		CH <sub>3</sub>	Im	Ring				
Fe <sup>I</sup> PorIm <sub>2</sub>	0.67	0.15	0.15	-0.97	-2.08	-	6.54	
Fe <sup>II</sup> CorIm <sub>2</sub> <sup>+</sup>	0.70	0.17	0.17	-0.04	-1.84	-	6.54	
Co <sup>I</sup> PorIm <sub>2</sub>	0.69	0.12	0.12	-0.92	-2.19	0.99	7.45	
Co <sup>II</sup> CorIm <sub>2</sub> <sup>+</sup>	0.72	0.13	0.13	0.01	-1.97	1.00	7.45	
Fe <sup>III</sup> PorIm <sub>2</sub> <sup>+</sup>	0.84	0.26	0.26	-0.36	-2.20	1.07	6.26	
Fe <sup>III</sup> CorIm <sub>2</sub> <sup>2+</sup>	0.85	0.27	0.28	0.60	-1.96	1.02	6.28	
Co <sup>III</sup> PorIm <sub>2</sub> <sup>+</sup>	0.72	0.30	0.30	-0.32	-2.12	-	7.30	
Co <sup>III</sup> CorIm <sub>2</sub> <sup>2+</sup>	0.73	0.31	0.31	0.64	-1.87	-	7.32	

**Table 9.** Mulliken charges, spin density, and 3d population on some atoms and groups of atoms the four-coordinate MCor/Por complexes.

Compound	charge on			spin on	M 3d
	M	Ring	4N <sub>eq</sub>	M	population
Fe <sup>I</sup> Por <sup>-</sup>	0.59	-1.59	-2.37	2.02	6.54
Fe <sup>I</sup> Cor	0.62	-0.62	-2.10	1.94	6.58
Co <sup>I</sup> Por <sup>-</sup>	0.51	-1.51	-2.33	0.89	7.55
Co <sup>I</sup> Por <sup>-a</sup>	0.38	-1.38	-2.24	-	7.72
Co <sup>I</sup> Cor	0.50	-0.50	-2.05	0.63	7.64
Co <sup>I</sup> Cor <sup>a</sup>	0.42	-0.42	-1.98	-	7.74
Fe <sup>II</sup> Por	0.66	-0.66	-2.41	2.04	6.47
Fe <sup>II</sup> Cor <sup>+</sup>	0.74	0.26	-2.16	2.09	6.49
Co <sup>II</sup> Por	0.64	-0.64	-2.33	1.10	7.49
Co <sup>II</sup> Cor <sup>+</sup>	0.68	0.32	-2.09	1.10	7.50

<sup>a</sup> Closed-shell singlet state.

**Table 10.** Calculated reduction potentials for the MCor/PorIm<sub>2</sub>, MCor/PorImMe, and the four-coordinate MCor/Por complexes.

Axial ligands: Complex	Im <sub>2</sub>			Im-Me			-		
	= 1	= 4	= 80	= 1	= 4	=	= 1	= 4	=
						80			80
CoPor	0.08	-0.69	-1.03	-3.96	-2.84	-2.29	-3.78	-2.53	-1.84
FePor	0.39	-0.38	-0.72	-3.81	-2.65	-2.05	-3.54	-2.43	-1.87
CoCor	3.26	0.56	-0.72	-0.98	-1.82	-2.20	-0.31	-1.14	-1.48
FeCor	3.53	0.84	-0.42	-0.52	-1.32	-1.67	-0.19	-1.11	-1.52

**Table 11.** Calculated inner-sphere reorganisation energies (kJ/mol) for the MCor/PorIm<sub>2</sub> (DZpdf/6-31G\* basis set) and MCor/PorImMe (TZPP basis set) complexes.

Complex	ox	red	
FePorIm <sub>2</sub>	5	4	8
FeCorIm <sub>2</sub>	5	4	9
CoPorIm <sub>2</sub>	105	74	179
CoCorIm <sub>2</sub>	114	82	197
FePorImMe	3	1	5
FeCorImMe	6	3	9
CoPorImMe	6	6	13
CoCorImMe	18	11	29

**Table 12.** Co-C BDEs (kJ/mol) for the MCor/PorImMe complexes, calculated with the DZpdf/6-31G(d) basis set.

<b>Complex</b>	<b>BDE</b>		
	= 1	= 4	= 80
FePorImMe	146.7	144.2	142.7
FeCorImMe	148.0	147.5	147.6
CoPorImMe	156.4	153.4	151.5
CoCorImMe	158.6	157.7	157.5

**Table 13.** Hydrolysis energies (kJ/mol), Eqn. (3), for the MCor/PorImMe complexes, calculated with the DZpdf/6-31G(d) basis set.

<b>Complex</b>	<b>Energy</b>		
	= 1	= 4	= 80
FePorImMe	-121.2	-117.8	-117.6
FeCorImMe	-122.2	-115.3	-112.4
CoPorImMe	-72.7	-75.4	-78.9
CoCorImMe	-75.5	-71.8	-70.7

**Table 14.** Methyl-transfer energies (kJ/mol), Eqn. (5), for the MCor/PorImMe complexes, calculated with the DZpdf/6-31G(d) basis set.

<b>Complex</b>	<b>Energy</b>		
	= 1	= 4	= 80
FePorImMe	-149.4	-74.8	-135.2
FeCorImMe	-436.0	-176.0	-147.4
CoPorImMe	-127.6	-96.6	-145.2
CoCorImMe	-416.9	-163.0	-139.4



**Figure 1.** The porphyrin (left) and corrin (right) ring systems.

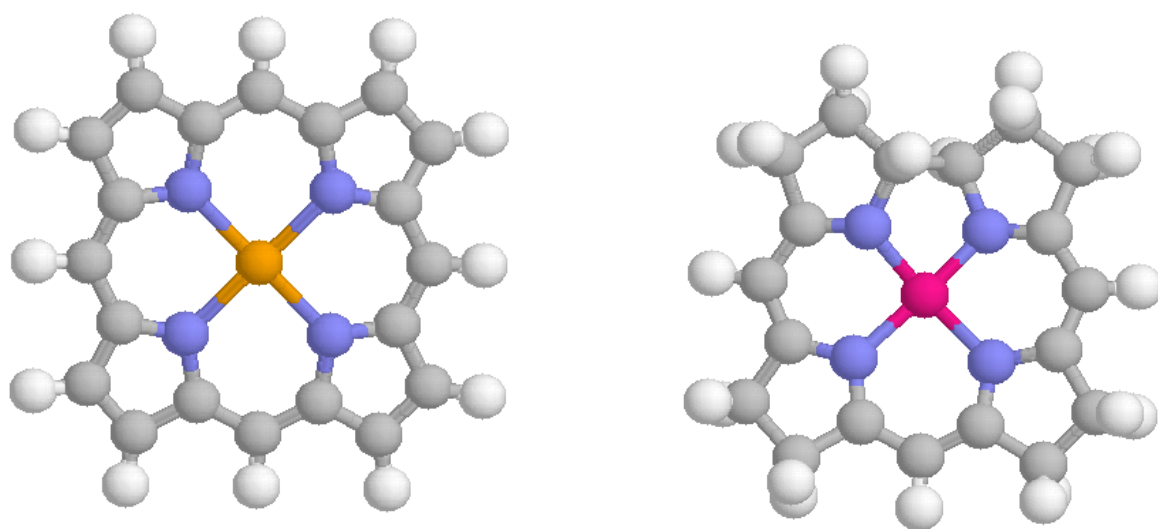
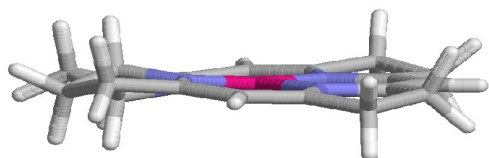
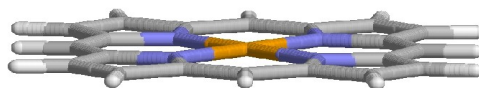


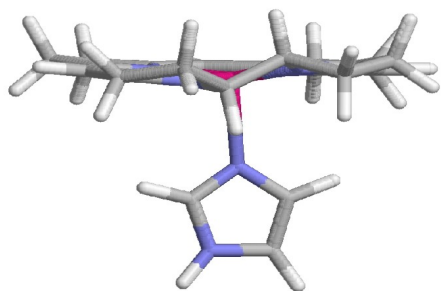
**Figure 2.** Optimised structures of the studied CoCor and FePor complexes.



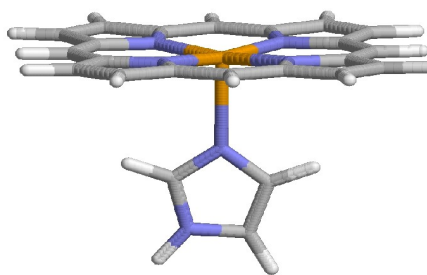
$\text{Co}^{\text{I}}\text{Cor}$



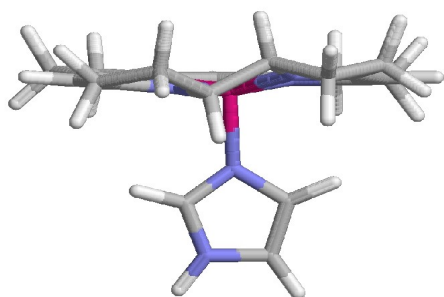
$\text{Fe}^{\text{I}}\text{Por}$



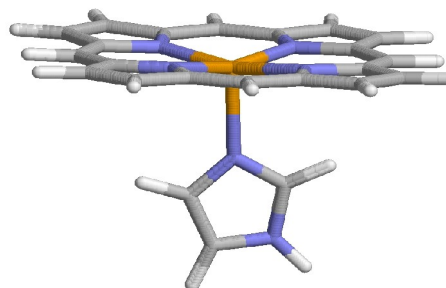
$\text{Co}^{\text{II}}\text{CorIm}$



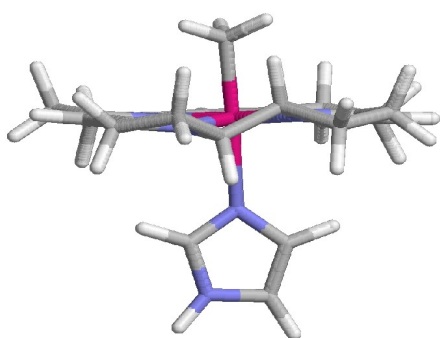
$\text{Fe}^{\text{II}}\text{PorIm}$



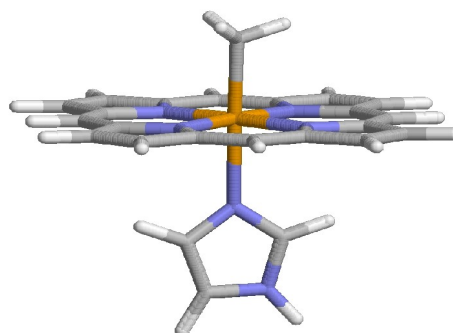
$\text{Co}^{\text{III}}\text{CorIm}$



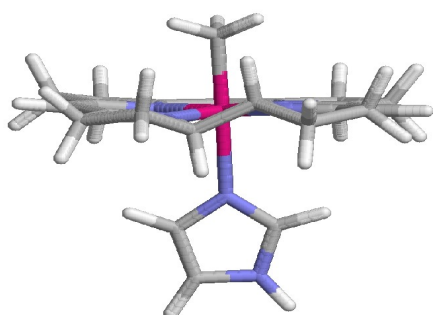
$\text{Fe}^{\text{III}}\text{PorIm}$



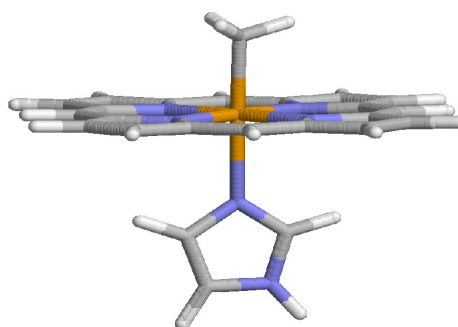
Co<sup>II</sup>CorMeIm



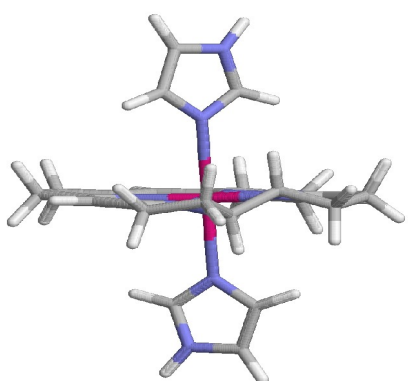
Fe<sup>II</sup>PorMeIm



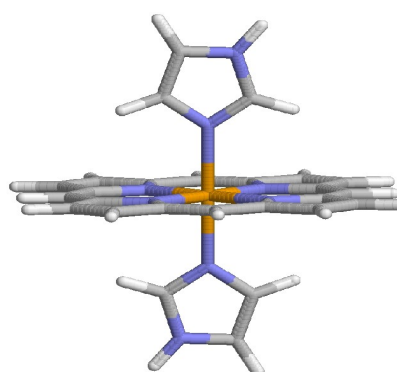
Co<sup>III</sup>CorMeIm



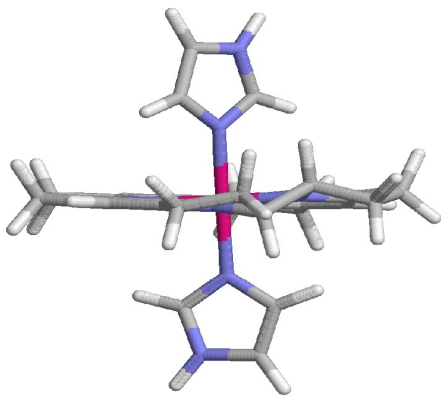
Fe<sup>III</sup>PorMeIm



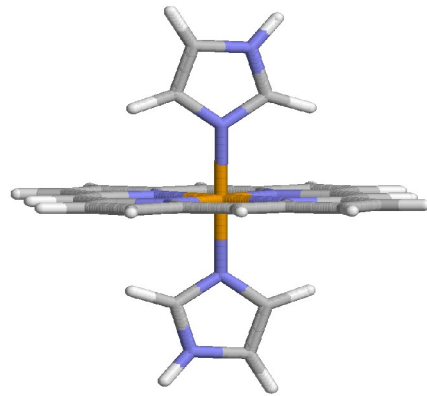
Co<sup>II</sup>CorIm<sub>2</sub>



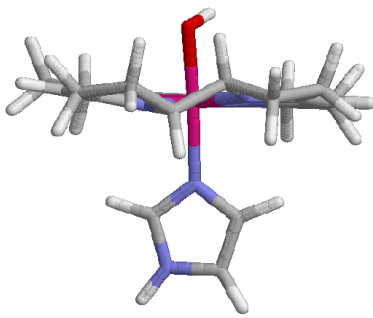
Fe<sup>II</sup>PorIm<sub>2</sub>



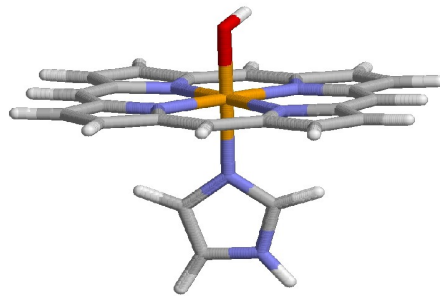
$\text{Co}^{\text{III}}\text{CorIm}_2$



$\text{Fe}^{\text{III}}\text{PorIm}_2$

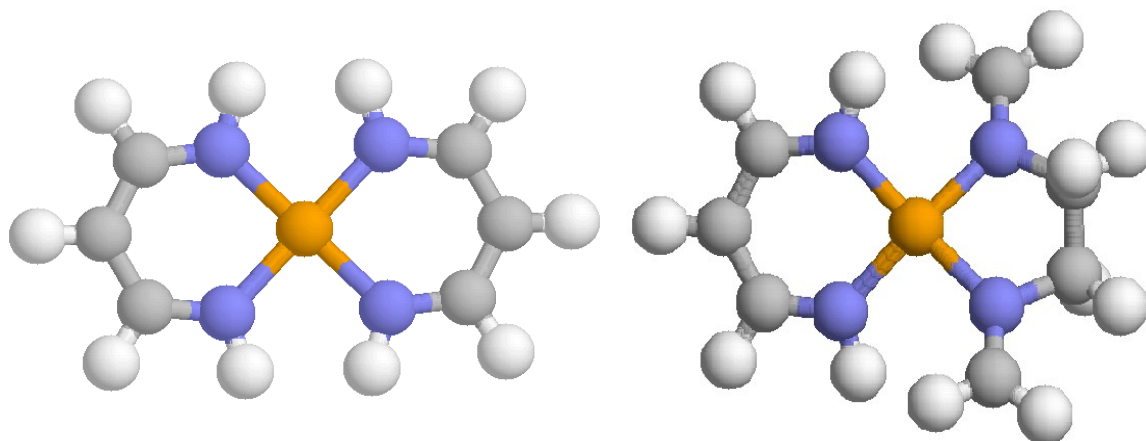


$\text{Co}^{\text{III}}\text{CorImOH}$



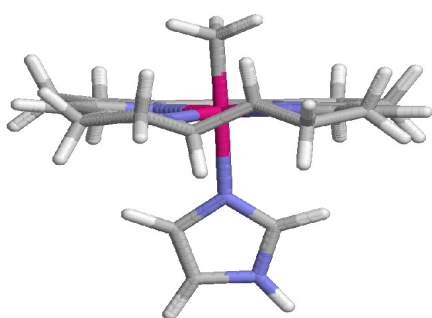
$\text{Fe}^{\text{III}}\text{PorImOH}$

**Figure 3.** The  $M(\text{NH}(\text{CH})_3\text{NH})_2$  (left) and  $M(\text{NH}(\text{CH})_3\text{NH})(\text{CH}_2\text{NH}(\text{CH})_2\text{NHCH}_2)$  (right) models with removed ring strain.



### **Text for Table of contents**

Density functional calculations have been used to compare geometric, electronic, and functional properties of iron and cobalt porphyrins and corrins using models of the type shown to the left. Corrin stabilises low-spin Co and gives strong Co-C bonds, whereas Fe gives low reorganisation energies.



(The figure can be reproduced in colour or black and white)